



## Light-responsive nanozymes for biosensing

Cite this: *Analyst*, 2020, **145**, 4388Yufeng Liu, <sup>a</sup> Xiaoyu Wang <sup>a</sup> and Hui Wei <sup>\*,a,b</sup>

Received 24th February 2020,

Accepted 23rd April 2020

DOI: 10.1039/d0an00389a

rsc.li/analyst

Using light as an external stimulus plays a key role not only in modulating activities of nanozymes, but also in constructing efficient biosensing systems. This mini-review highlights recent advances in light-responsive nanozyme-based biosensing systems. First, we introduce the light stimulation for regulating nanozymes' activities. Then, several strategies are presented to construct efficient photo-responsive nanozyme-based detection systems by using metal-based nanozymes, carbon-based nanozymes, and MOF-based nanozymes, respectively. Moreover, the detection mechanisms of current biosensors are discussed. Finally, we discuss the current challenges and future perspectives of this research area.

## 1. Introduction

Nanozymes, as emerging artificial enzymes, not only exhibit enzyme-like catalytic properties, but also have their intrinsic advantages over natural enzymes (such as low cost, high stability, and large-scale production). Furthermore, they are superior to conventional enzyme mimics in multi-functionalities and in activities that can be modulated.<sup>1–8</sup> The latter allow us to modulate the activities of nanozymes *via* various strategies. Among them, light stimulation is of great interest because of its high efficiency and spatial controllability.<sup>9–14</sup> Moreover, light stimulation is also a fascinating regulation of natural enzymes,<sup>15–17</sup> such as DNA photolyase,<sup>18</sup> fatty acid photodecarboxylase,<sup>19</sup> and protochlorophyllide oxidoreductase.<sup>20</sup> In this regard, the introduction of light-responsive functionalities will be a promising way to design new enzyme mimics (including nanozymes) for further applications.

Nanomaterials with light harnessing capacity can utilize solar energy in numerous fields,<sup>9,21–23</sup> including photovoltaic industry,<sup>24</sup> fuel generation,<sup>25,26</sup> environmental protection,<sup>27</sup> *etc.* Most of these photoactive nanomaterials have the photo-induced electron transfer (PET) ability,<sup>28,29</sup> which is a fundamental process of photocatalytic reactions. Therefore, modulating the interactions between substrates and active electrons can produce on-demand effects.<sup>30–32</sup> The currently developed light-responsive nanozymes can be mainly classified into two

types: for type I, the photocatalytic properties originate from the nanomaterials themselves, which could generate reactive oxygen species (ROS) by absorbing light and subsequently oxidizing enzymatic substrates; for type II, the photocatalytic activities are entirely from functional photoactive molecules which are modified on the nanomaterials. For instance, photoisomerization,<sup>33</sup> photo-induced pH changes,<sup>34</sup> and photothermal effects<sup>35</sup> can impact the enzyme-like activities of non-photoactive nanozymes. By taking advantages of the two types of photo-responsive nanozymes, lots of applications, including biosensing, degradation of organic pollutants,<sup>36–38</sup> modification of DNA,<sup>39,40</sup> and anti-bacteria,<sup>41–44</sup> have been developed. With the rapid development of this area, two recent comprehensive reviews<sup>45,46</sup> on light-activated nanozymes have been published, whereas none of them focused on the strategies to construct photoactive nanozyme-based biosensors.

To highlight the strategy of using light-activated nanozymes for building biosensing systems, in this mini-review, we first introduced the activity modulation of nanozymes under light stimulation. Then, several types of nanozymes with light-induced enzyme-like activities were systematically presented for developing the photoactive sensing systems. Subsequently, the mechanisms of detection towards the above-mentioned sensing systems were summarized. Finally, we discuss the current challenges of the photoactive nanozymes and further propose several perspectives of light-responsive biosensing systems for future applications.

## 2. Light stimulation for modulating the activities of nanozymes

As mentioned above, there are two types of light-responsive nanozymes. For type I, ROS, such as superoxide anion ( $\text{O}_2^-$ ), hydroxyl radical ( $\text{OH}^\bullet$ ), singlet oxygen ( $^1\text{O}_2$ ), and photo-gener-

<sup>a</sup>Department of Biomedical Engineering, College of Engineering and Applied Sciences, Nanjing National Laboratory of Microstructures, Jiangsu Key Laboratory of Artificial Functional Materials, Chemistry and Biomedicine Innovation Center (ChemBIC), Nanjing University, Nanjing, Jiangsu 210093, China.  
E-mail: weihui@nju.edu.cn; http://weilab.nju.edu.cn; Fax: +86-25-83594648; Tel: +86-25-83593272

<sup>b</sup>State Key Laboratory of Analytical Chemistry for Life Science and State Key Laboratory of Coordination Chemistry, School of Chemistry and Chemical Engineering, Nanjing University, Nanjing, Jiangsu 210023, China

ated holes ( $h^+$ ), is involved during the photocatalytic reactions. The main advantage of photocatalytic nanozymes is their ability to catalyze challenging reactions that hardly proceed without light. However, the disadvantage of such nanozymes is the low efficiency under the sunlight, and thus a powerful light source such as a Xe lamp is needed. For type II, since these nanozymes themselves are non-photocatalytically active, photoactive molecules are needed to facilitate the photocatalysis. Unlike photocatalytic reactions, minimal side reactions are an advantage of this type of nanozymes because of the generation of less ROS, which is suitable for the construction of reversible reaction systems. Meanwhile, the limited amount and types of photoactive molecules are the main drawbacks of this kind of nanozymes. These two types of light-stimulated modulations including photocatalytic and non-photocatalytic are discussed in this section.

## 2.1. Photocatalytic modulation

Improving the production of ROS is a fundamental method for accelerating photocatalytic reactions.<sup>47–49</sup> To this end, improving the light absorption is a promising strategy to enhance the ROS yield. For example, although carbon-based photosensitizers<sup>50</sup> are one kind of attractive photoactive nanozymes, low efficiency and lack of rational design were the bottlenecks for the construction of highly efficient photo-oxidative nanozymes. To rationally design carbon-based photoactive nanozymes, in 2018, the Wu group synthesized a series of nitrogen-doped carbon dots (C-dots) and studied the correlation between photo-oxidation activity and phosphorescence quantum

yield.<sup>41</sup> As shown in Fig. 1A, the C-dots exhibited enzyme-like activity under light irradiation and the photo-generated ROS was used for antimicrobial chemotherapy. Further experimental results showed that C-dots exhibit better performance for the activation of oxygen than other carbon-based nanomaterials as well as dyes of phloxine B (PB) and rose bengal (RB) (Fig. 1B). To provide an insight into the production mechanism of singlet oxygen, Fig. 1C shows the correlation between fluorescence and phosphorescence of four types of C-dots. In addition, the oxidation efficiency of 3,3',5,5'-tetramethylbenzidine (TMB) indicated that the C-dots had a positive correlation between the phosphorescence quantum yield and the photosensitizing ability (Fig. 1D).

In addition, the long excited-state lifetime is another important factor of light-responsive nanozymes for increasing the yield of ROS. In this regard, the Liu group used Mn(II) to communicate with C-dots, which promoted the catalysis of C-dots for TMB oxidation at neutral pH in the presence of singlet oxygen produced *via* photosensitization (Fig. 2A).<sup>51</sup> Mn(II) can be oxidized to Mn(III) by the photo-generated singlet oxygen, enhancing the electron transfer upon light irradiation. Furthermore, compared with several other metal ions, only Mn(II) could enhance the oxidation of TMB in a physiological buffer (Fig. 2B). This Mn-mediated oxidation method solved a long-standing problem for the nanozymes in lacking the activity at physiological pH.

Hydroxyl radical is another kind of ROS in photocatalytic reactions. For example, the Xia group found gold nanoparticles (Au NPs) exhibited peroxidase-like activity under visible-light

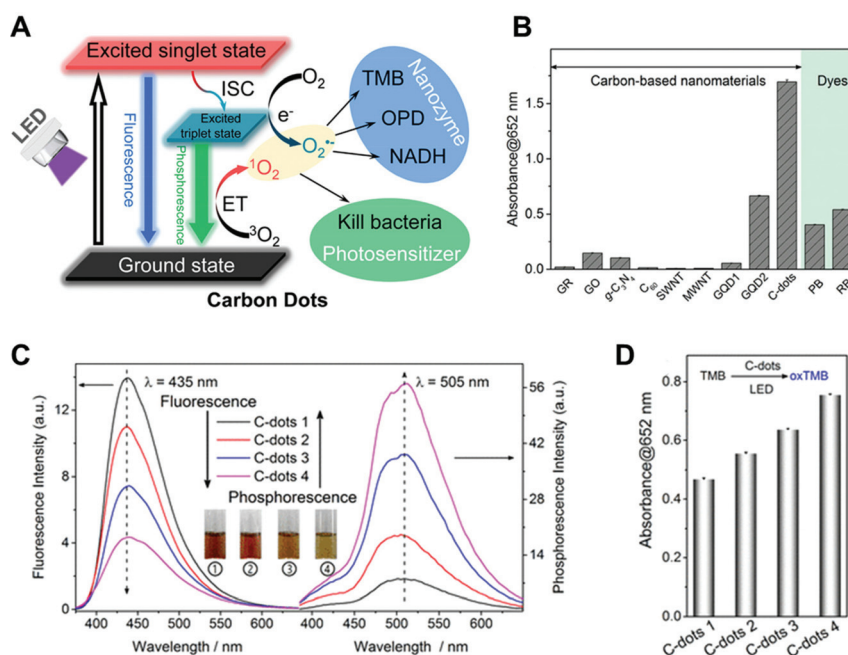


**Fig. 1** (A) Schematic illustration of photo-sensitized oxygen activation with C-dot nanozymes for photodynamic antimicrobial chemotherapy. (B) Comparison of the oxygen activation performance of various carbon-based nanomaterials and two molecular photosensitizers (PB and RB) for TMB oxidation under light. All the materials were of 5 mg L<sup>-1</sup>. (C) Fluorescence and phosphorescence (in the PVA matrix) spectra of four types of C-dots. Inset shows the solution of C-dots at different temperatures of synthesis. (D) TMB photo-oxidation efficiencies of the four C-dots. Reproduced from ref. 41 with permission from the American Chemical Society, copyright 2018.

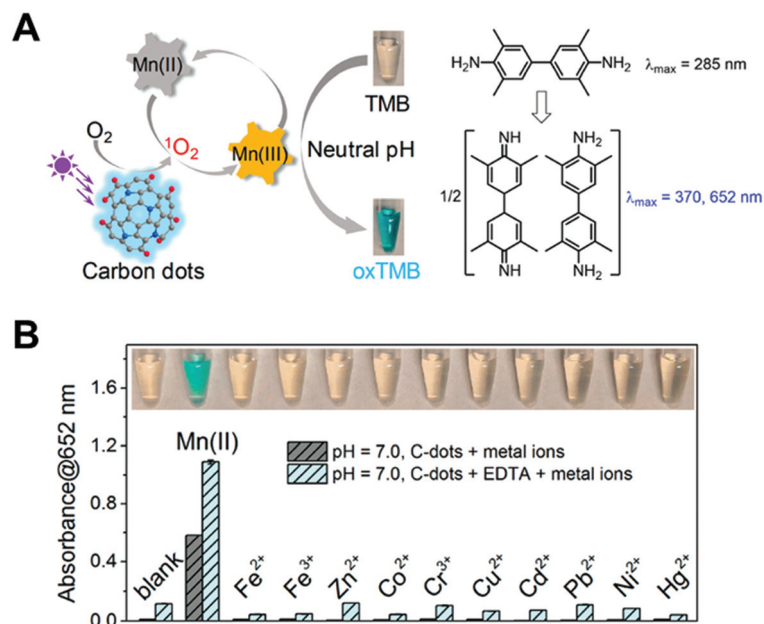


Fig. 2 (A) Schematic illustration of Mn(II) enhancing the photo-oxidase activity of C-dots at neutral pH. (B) Among the tested metals (1 mM each), without or with 1 mM EDTA, only Mn(II) enhanced oxidation. Reproduced from ref. 51 with permission from the American Chemical Society, copyright 2019.

irradiation.<sup>52</sup> Based on the unique localized surface plasmon resonance (LSPR) property of Au NPs, they revealed that upon LSPR excitation, hot carriers (electrons and holes) were activated on the surface of Au NPs. The injection of hot electrons into the H<sub>2</sub>O<sub>2</sub> molecule could produce more hydroxyl radicals, leading to an enhanced enzyme-like performance. Similarly, superoxide anion can be generated by the activation of oxygen through the injection of hot electrons. Apart from Au NPs, many photocatalytic nanozymes including *g*-C<sub>3</sub>N<sub>4</sub>,<sup>53</sup> Au-Pd-Bi<sub>2</sub>WO<sub>6</sub>,<sup>54</sup> and β-In<sub>2</sub>S<sub>3</sub><sup>55</sup> rely on the photo-generated superoxide anion for the oxidation of substrates.

## 2.2. Non-photocatalytic modulation

Unlike the photocatalytic regulation, non-photocatalytic modulation affects nanozymes' activity in the absence of ROS. As shown in Table 1, photoisomerization,<sup>56</sup> photo-induced pH change,<sup>57</sup> and photothermal effect<sup>58</sup> are the currently developed strategies for activity regulation. In 2017, the Qu group reported that a photoactive molecule of azobenzene (Azo) with the ability of light-driven isomerization reversibly regulated the catalase-like activity of Au nanoparticles (NPs) (Fig. 3A).<sup>59</sup> They used Azo-modified mesoporous silica as a host to encapsulate Au NPs and cyclodextrin (CD) (Au-Si-Azo).

The *trans* conformations of Azo in Au-Si-Azo led to catalytic site blockage by CD, and subsequently inhibited the catalytic activity. As shown in Fig. 3B, under the irradiation of UV light, azo undergoes the isomerization from *trans* to *cis* conformation, which enhanced the enzyme-like activity of Au NPs. However, after the visible light irradiation, transformation of azo from *cis* to *trans* conformation took place, CD was unable to be released and the catalase-like activity of Au NPs was inhibited (Fig. 3C). Inspired by this, the Qu group further developed an azo-modified Pd nanozyme and controlled its catalytic activity by the light-induced isomerization.<sup>60</sup> Likewise, the Prins group reported that the hydrolysis activity of Au NPs can be reversibly regulated by switching the light source.<sup>61</sup> The Au NPs were functionalized with a monolayer of C<sub>9</sub>-thiol-based molecules to have a higher affinity towards the *trans* isomer of the photoactive molecule. Therefore, the photoactive molecule with the *trans* conformation inhibited the absorption of the substrate 2-hydroxypropyl-4-nitrophenylphosphate (HPNPP) and thus decreased the hydrolysis activity. Upon irradiation at 365 nm, the *trans* isomer of photoactive molecule transformed into *cis* isomer, lowering their affinity on the surface of Au NPs.

Table 1 Non-photocatalytic modulations of light-responsive nanozymes

Modulator	Mechanism	Nanozymes	Activity	Ref.
Azobenzene	Photoisomerization	Au-Si-Azo	Catalase-like activity	59
Azobenzene	Photoisomerization	CASP	Bioorthogonal catalysis	60
Azobenzene	Photoisomerization	Au NP	Transphosphorylation	61
2-Nitrobenzaldehyde	Photoacid effect	Nanoceria	Oxidase-like activity	63
2-Nitrobenzaldehyde	Photoacid effect	MoS <sub>2</sub>	Gram-selective antimicrobial	64
Au NPs	Photothermal effect	Au@HCNs	ROS production	65

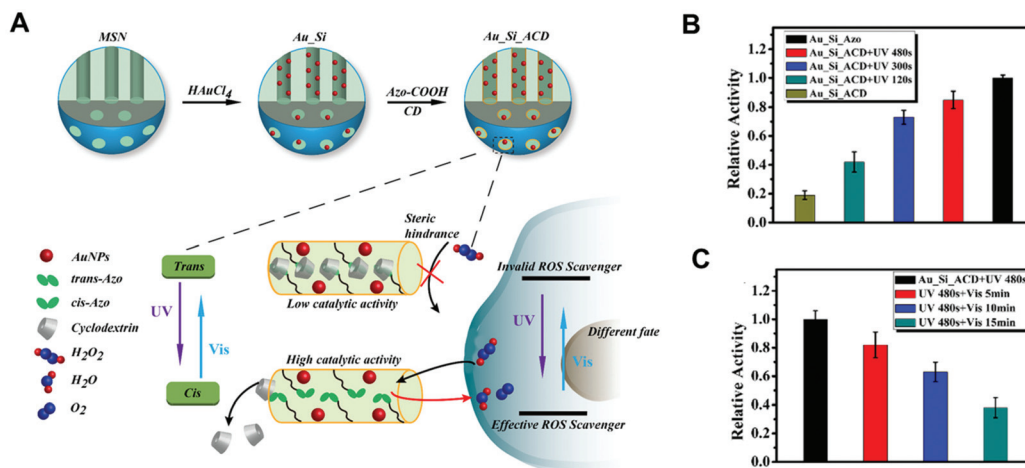


**Fig. 3** (A) Synthetic procedure for Au\_Si\_ACD. The UV and visible light reversibly regulate the catalytic activity of Au\_Si\_ACD by the *trans*–*cis* photoisomerization of Azo molecules to control the host–guest interactions between Azo and CD. The new nanozymes can act as a controllable ROS scavenger in cells with different catalytic activities. (B) Au\_Si\_ACD was irradiated with UV light for 0, 120, 300 and 480 s and then incubated with H<sub>2</sub>O<sub>2</sub> for 60 min. The catalase-like activity was normalized to that of Au\_Si\_Azo sample. (C) After irradiation with UV light for 480 s, Au\_Si\_ACD was exposed under visible light for 5, 10 and 15 min. The catalase-like activity was normalized. Reproduced from ref. 59 with permission from John Wiley and Sons, copyright 2017.

Meanwhile, the transphosphorylation rate of HPNPP was upregulated.

Besides modifying with photo-isomerized molecules, the combination with a photoacid molecule is another way to fabricate photo-responsive nanozymes. A photoacid molecule can induce pH change during the light irradiation, further regulating the pH-dependent activity of nanozymes. In this regard, a typical photoacid molecule of 2-nitrobenzaldehyde (2-NBA)<sup>62</sup> was applied to activate the enzyme-like activity of nanoceria<sup>63</sup> nanozyme (Fig. 4A) and increase the antimicrobial<sup>64</sup> activity of MoS<sub>2</sub> nanozyme (Fig. 4B). In addition, nanozymes' activity could also be modulated by the photothermal effect. For

instance, Au NPs could improve the production of photo-generated ROS by increasing the photothermal effect, which benefited cancer therapy (Fig. 4C).<sup>65</sup>

### 3. Construction of biosensing systems using light-responsive nanozymes

Using a light-controllable system for biosensing is a promising analytical method in recent years.<sup>66–69</sup> To date, various photo-

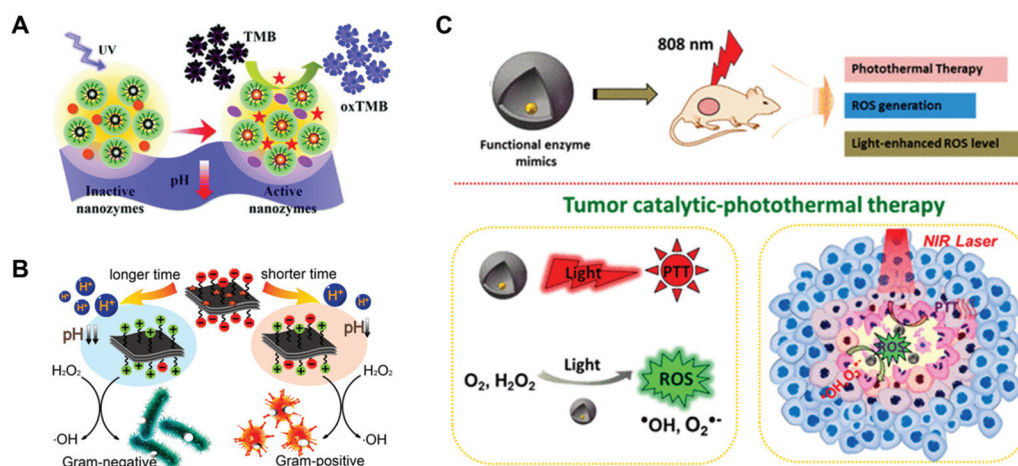


**Fig. 4** Schematic illustrations of controllable oxidase-like activity of dextran-decorated nanoceria based on the photo-induced proton release (A), light-modulated nanozyme of MoS<sub>2</sub> for a Gram-selective antimicrobial (B), and the catalytic–photothermal tumor therapy with yolk–shell Gold@Carbon nanozymes (C). (A) Reproduced from ref. 63 with permission from the Royal Society of Chemistry, copyright 2018. (B) Reproduced from ref. 64 with permission from the American Chemical Society, copyright 2018. (C) Reproduced from ref. 65 with permission from the American Chemical Society, copyright 2018.



active materials have been applied for the detection of many analytes, such as ions,<sup>70</sup> thiols,<sup>71</sup> and amino acids.<sup>72</sup> These photo-responsive systems have several advantages. First, the pre-mixture of an inactive sensor and an analyte will not affect the performance of their active state, thus avoiding the overestimation of detection. For instance, the Hecht group has developed a methodology for the detection of amines using specific diarylethenes (DAEs), which can be activated not only on the defined areas by using light irradiation, but also in the desired point of time.<sup>73</sup> Therefore, the influence of local concentration can be avoided. Second, the light-controllable detection system possesses high sensitivity and low background since the separation of signal excitation and detection, such as the analytical method of photoelectrochemistry.<sup>74</sup> Third, the photoactive system is of great advantage for the detection upon cellular context due to the ready conversion from an inert to active state, the short half-life time, and the self-quenching ability. For instance, the Spitale group introduced a novel strategy for measuring the RNA solvent accessibility called light-activated structural examination of RNA (LASER). Due to the exquisite sensitivity of LASER probing, the understanding of the transition structure of RNA is more accurate and faster.<sup>75</sup> With this in mind, in this section, the light-responsive nanozymes for the detection of biomolecules were systematically summarized and discussed based on the different types of nanozymes, including metal-, carbon-, and MOF-based ones.

### 3.1. Using metal-based nanozymes

**3.1.1. Metal halides.** In 2014, chitosan (CS)-modified silver halide NPs (AgX, X = Cl, Br, I) with light-responsive oxidase-like activities were developed by the Wang group for cancer cell detection.<sup>76</sup> A 500 W Xe lamp with a cut-off filter ( $\lambda \geq$

420 nm) was applied as the irradiation source. CS-AgX NPs could oxidize three colorless enzymatic substrates (*i.e.*, 3,3',5,5'-tetramethylbenzidine (TMB), *o*-phenylenediamine (OPD), and 2,2'-azino-bis(3-ethylbenzothiazoline-6-sulfonic acid (ABTS)) to their colored products upon irradiation (Fig. 5A). Kinetic studies of oxidizing TMB suggested a ping-pong catalytic mechanism of CS-AgX NPs. Moreover, the excellent oxidase-like activity was retained over a broad pH range (3.0–7.0) (Fig. 5B). In addition, mechanistic studies indicated that the photo-generated  $\cdot\text{O}_2^-$  and holes were the reactive intermediates for oxidizing TMB. Subsequently, CS-AgI NPs were modified with folic acid (FA) *via* the formation of an amide bond between FA and CS. The as-prepared FA-CS-AgI was employed for cancer cell detections as folate receptors were usually overexpressed on cancer cell membranes (Fig. 5C). Therefore, different types of cancer cells were detected according to their different numbers of folate receptors (Fig. 5D).

**3.1.2. Metal.** Because of the unique optical property of noble-metal NPs, several noble metal-based light-responsive sensing systems were explored. In 2015, the Wang group used bovine serum albumin (BSA) to stabilize Au nanoclusters to control their size-dependent optical properties.<sup>77</sup> With the help of BSA, the obtained BSA-Au NCs exhibited excellent oxidase-like activities under visible light irradiation. Since trypsin can digest BSA and decrease the catalytic activity of BSA-Au-NCs, a facile colorimetric sensing system for trypsin was developed (Fig. 6A). The photoactive trypsin sensing platform showed excellent selectivity and a limit detection of  $0.6 \mu\text{g mL}^{-1}$  (Fig. 6B and 6C). Inspired by this, the Wu group developed an ascorbic acid (AA)-regulated  $\text{Ag}_3\text{PO}_4$  nanozyme for multiple biological detections.<sup>78</sup>  $\text{Ag}^+$  on the surface of

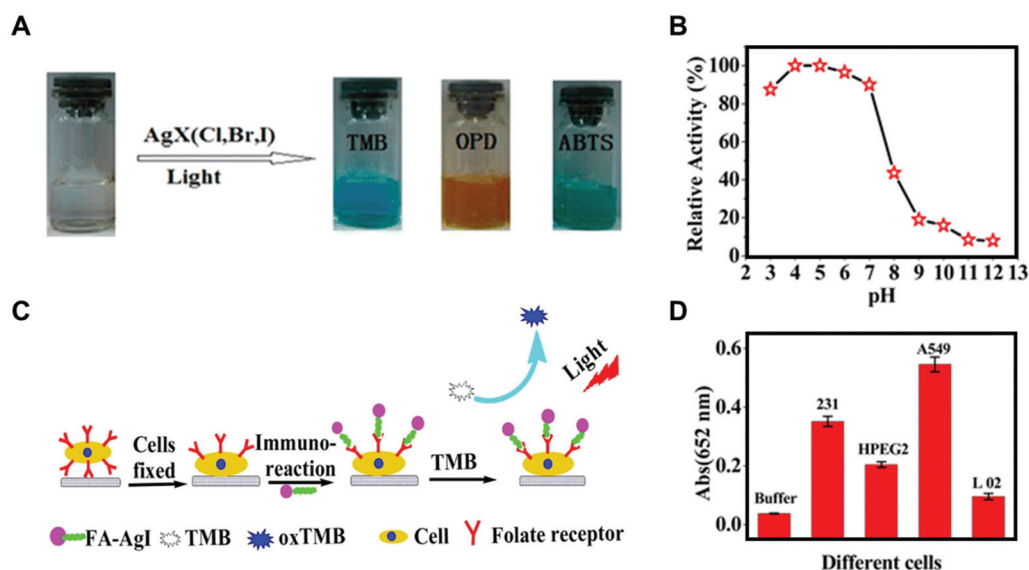
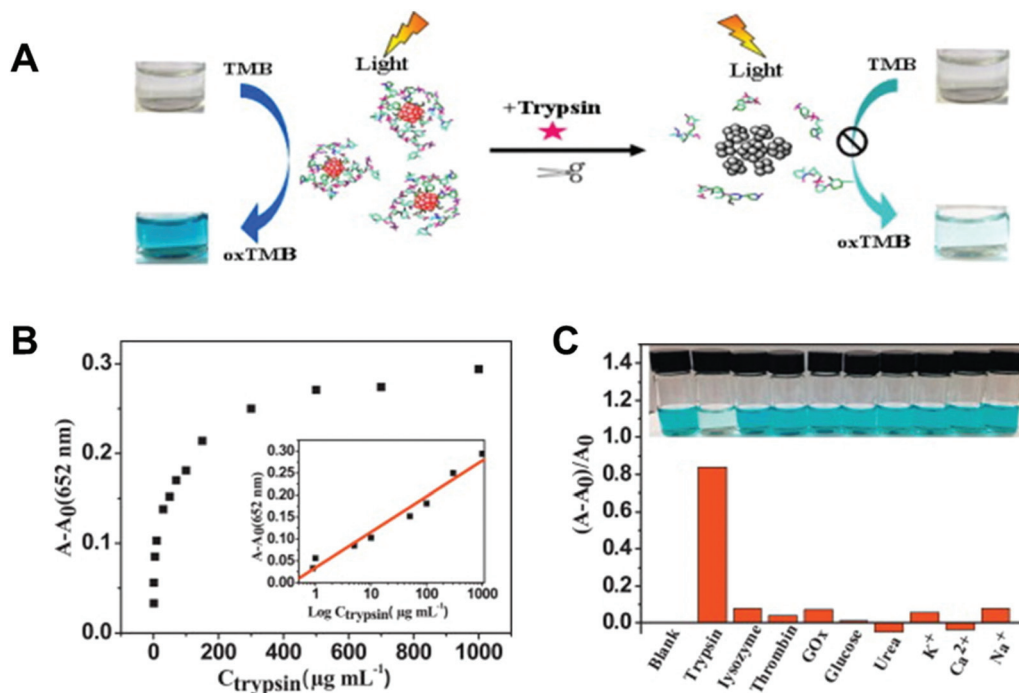


Fig. 5 (A) Color evolution of TMB, OPD, and ABTS oxidation by visible light-stimulated CS-AgX (X = Cl, Br, I). (B) Relative catalytic activity of the CS-AgI NPs under visible light irradiation ( $\lambda \geq 420$  nm) at a range of different solution pH values. (C) Proposed process of cancer cell detection by using FA-CS-AgI. (D) Response of different cells using FA-CS-AgI to TMB under visible light irradiation. The error bars represent the standard deviation of five measurements. Reproduced from ref. 76 with permission from the American Chemical Society, copyright 2014.



**Fig. 6** (A) Schematic representation of the colorimetric sensing mechanism for trypsin based on the enzyme-like activity of BSA–Au NCs. (B) Change in absorption and the linear relationship (inset shows the curve) between  $(A - A_0)$  of oxTMB at 652 nm and the concentration of trypsin. (C) The effect of different substances on the colorimetric detection of trypsin. Reproduced from ref. 77 with permission from Elsevier, copyright 2015.

$\text{Ag}_3\text{PO}_4$  NPs can be reduced by AA to form a  $\text{Ag}^0/\text{Ag}_3\text{PO}_4$  heterostructure, which in turn enhanced its oxidase-like activities due to the effect of surface plasmon resonance (SPR). Therefore, AA and AA-related biomolecules were detected using this photo-responsive sensing system.

**3.1.3. Metal oxides.** Besides the noble metal nanomaterials, metal oxide nanomaterials such as  $\text{TiO}_2$  NPs could be used for photoactive sensing as well. In 2015, the Wang group reported that coordinating CA on  $\text{TiO}_2$  NPs<sup>79</sup> extended their absorption range from ultraviolet to visible, which activated the oxidase-like activity of  $\text{TiO}_2$  NPs under visible light stimulation (Fig. 7A). Upon light irradiation,  $\text{TiO}_2$ -CA NPs exhibited a typical Michaelis–Menten kinetics, and the activity could be easily controlled by switching “on/off” state of light. In this way, CA correlated biomolecules including alkaline phosphatase (ALP) and ALP inhibitor were effectively detected. Later, another photoactive peroxidase mimic was constructed by using dihydroxyphenylalanine (DOPA) to coordinate with  $\text{TiO}_2$  NPs<sup>80</sup> (Fig. 7B). The DOPA- $\text{TiO}_2$  nanozyme produced more reactive species than the non-coordinated  $\text{TiO}_2$  NPs under visible light irradiation. Subsequently, since tyrosinase (TYR) could catalyze tyrosine to generate DOPA, the  $\text{TiO}_2$  NP-based photoactive sensor was applied for TYR detection.

### 3.2. Using carbon-based nanozymes

**3.2.1. GO.** Another typical photoactive nanozyme was a carbon-based nanomaterial. In 2014, chitosan functional gra-

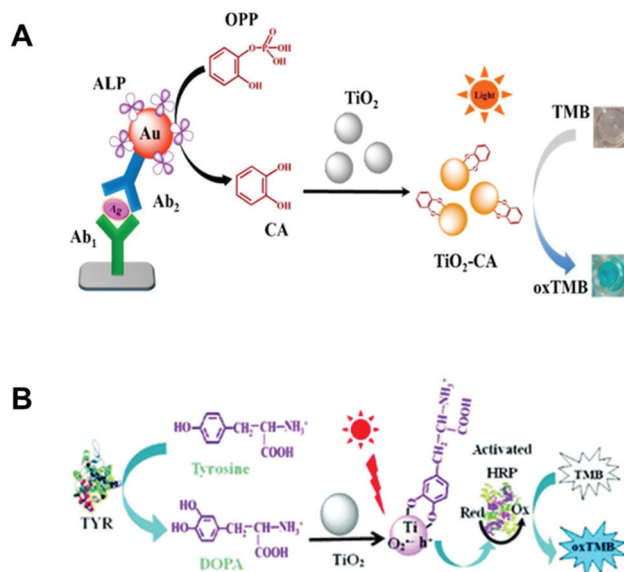


**Fig. 7** (A) Proposed immunodetection process for mouse IgG by coupling the *in situ*-generated photo-responsive nanozyme of CA- $\text{TiO}_2$ . (B) Schematic illustration of the colorimetric sensing mechanism for TYR based on the photoactive sensor. (A) Reproduced from ref. 79 with permission from the American Chemical Society, copyright 2015. (B) Reproduced from ref. 80 with permission from the Royal Society of Chemistry, copyright 2017.

phene oxide (CS-GO)<sup>81</sup> was shown to exhibit oxidase-like activity under visible light irradiation (Fig. 8A). Kinetics and mechanistic studies indicated that the CS-GO nanozyme possessed higher affinity towards TMB than HRP and the photo-generated holes ( $h^+$ ) represented the active species in TMB oxidation. Interestingly, the photo-responsive activity of CS-GO can be inhibited through the aggregation of GO, which was induced by the interaction between CS and concanavalin A (Con A). Meanwhile, glucose could compete against CS for interacting with Con A, which led to the recovery of the enzyme-like activity. Therefore, a selective and sensitive photo-stimulated sensing system was developed by CS-GO nanozymes for the detection of glucose (Fig. 8B).

**3.2.2.  $C_3N_4$ .** To further functionalize the carbon-based nanozymes, a photoactive sensing system by combining acid phosphatase (ACP) with  $C_3N_4$  was established.<sup>82</sup> ACP can hydrolyze pyrophosphate (PPi) to liberate copper ion ( $Cu^{2+}$ ), which subsequently triggers  $C_3N_4$  nanosheets to generate the enzyme-like activity under light irradiation. Switching “on/off” state of light can easily control the activity of  $Cu^{2+}/C_3N_4$ . Moreover, ACP can be effectively detected *via* this photoactive sensing system.

Besides, another carbon-based photoactive sensing system has been developed by the Choi group in 2019.<sup>83</sup> The  $C_3N_4$  nanozyme modified with KOH and KCl possessed excellent

glucose oxidase (GOx)-like activity under the light stimulation, which could catalyze glucose to produce  $H_2O_2$  (Fig. 8C). With the help of *in situ* generated  $H_2O_2$ , the  $C_3N_4$  nanozyme oxidized TMB *via* the HRP-like activity under dark conditions. By taking such advantages of the  $C_3N_4$  nanozyme, a cascade photoactive biosensor was developed for the detection of glucose. Moreover, using a microfluidic device could highly accelerate such biosensing processes, enabling the real-time monitoring of glucose with a detection limit of  $0.8\ \mu M$  in 30 s (Fig. 8D).

### 3.3 Using MOF-based nanozymes

To overcome the limited absorbance of photoactive nanomaterials under visible light, recently, a photo-sensitized MOF (PSMOF) has been reported as an oxidase mimic for biomedical applications by our group (Fig. 9A).<sup>84</sup> An organic dye of  $Ru(bpy)_3^{2+}$  with a stronger visible-light absorption<sup>85</sup> was used as a PS linker for the construction of PSMOF. The PSMOF showed excellent oxidase-like activity under light irradiation, and the enzyme-like activity could be controlled by switching light on and off. Mechanistic studies indicated that the dissolved oxygen could be activated by the PSMOF under light irradiation to form ROS including  $\cdot O_2^-$  and  $\cdot OH$ . Based on the production of ROS, the PSMOF nanozyme was used to detect

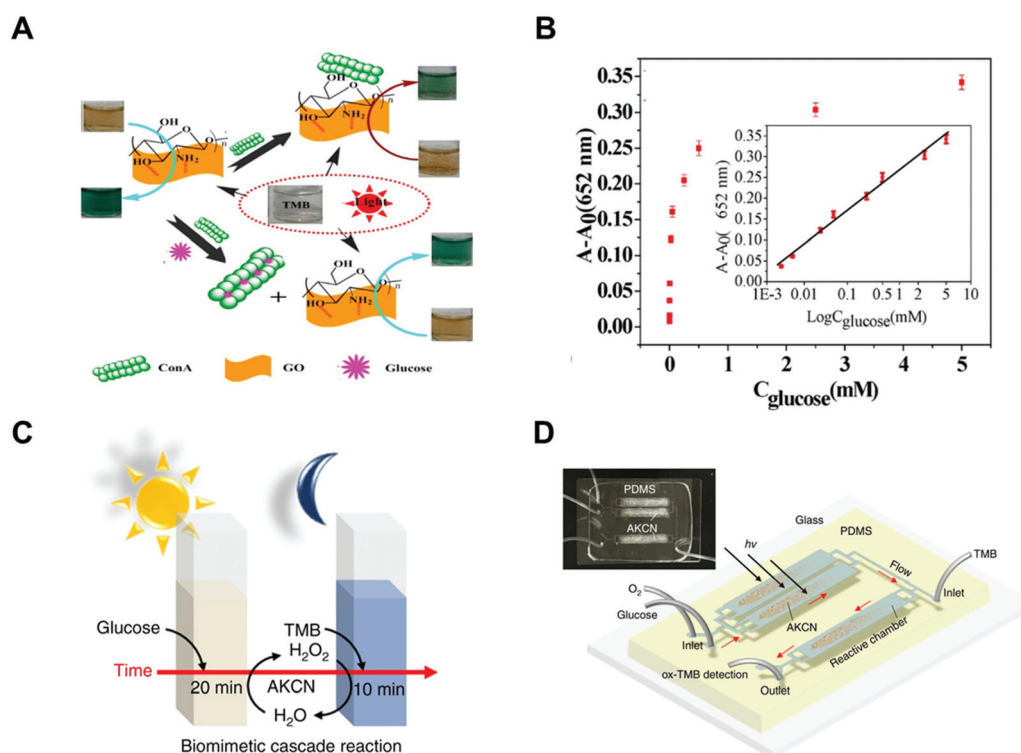


**Fig. 8** (A) Fabrication process and detection principle of the system to detect glucose. (B) Linear relationship between  $(A - A_0)$  of oxTMB at 652 nm and the concentration of glucose. (C) Scheme of the cascade reaction with continuous  $O_2$ -purging in a batch mode. (D) Scheme of the cascade reaction in a microfluidic device and the actual device image (inset). (A and B) Reproduced from ref. 81 with permission from the American Chemical Society, copyright 2014. (C and D) Reproduced from ref. 83 with permission from Springer Nature, copyright 2019.

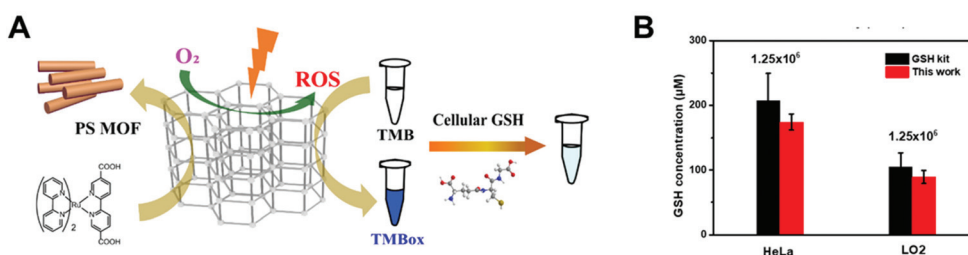


**Fig. 9** (A) Schematic illustration of the cellular GSH detection by using a PS MOF-based photoactive sensor. (B) Qualitative evaluation of cellular GSH levels with the developed sensor and a GSH kit. The number marked on the histogram is the cell density. Each error bar shows the standard deviation of three independent measurements. Reproduced from ref. 84 with permission from the American Chemical Society, copyright 2019.

the reducing molecule of glutathione in both normal and cancer cells (Fig. 9B).

## 4. Detection mechanisms

As mentioned above, most of the photoactive sensing systems were based on the following two sensing mechanisms. One was that the analytes affect the activity of the photo-responsive nanozymes by non-ROS-involved interactions. Therefore, the detection is mainly based on the effects of analytes on the photoactivity of nanozymes. For example, ACP could catalyze the hydrolysis of PPI to liberate  $Cu^{2+}$  and the released  $Cu^{2+}$  in turn enhances the photo-responsive enzyme-like activity of  $C_3N_4$  nanozyme. In this way, ACP could be detected by monitoring such variations of enzyme-like activity and the detection limit was  $8.8 \times 10^{-3} \text{ U L}^{-1}$ .<sup>82</sup> On the other hand, due to the correlation between photoactivity and light absorption ability, analytes with the ability of affecting the light absorbance of nanozymes could be detected. For instance, BSA-stabilized Au NCs endowed themselves with the ability of light absorption and exhibited enzyme-like activities under visible light irradiation. As the TYR could decrease the light absorption ability of BSA-Au NCs through the digestion of BSA, TYR could be detected by measuring the reduction of their enzyme-like activities.<sup>80</sup>

The other principle of sensing is based on ROS-mediated interactions, meaning the analytes need to be reacted with photo-generated ROS. Due to the strong oxidizing ability of ROS, biomolecules with reductive activity could be detected such as glutathione (GSH). However, the selectivity of this reaction is limited. For example, the reductive molecules of ascorbic acid (AA) and cysteine could interfere the detection of GSH.<sup>84</sup> Therefore, constructing more specific ROS-involved photosensing systems is of great interest. Recently, glucose could be oxidized to generate hydrogen peroxide by the modified  $C_3N_4$  nanozyme under light irradiation, demonstrating the glucose oxidase-like activity of  $C_3N_4$  nanozymes. Since the modified  $C_3N_4$  nanozyme also exhibited peroxidase-like activity, glucose could be detected by exploring the  $C_3N_4$  nanozyme-catalyzed GOx- and peroxidase-like cascade reactions.<sup>83</sup>

## 5. Conclusions and future perspectives

In this mini-review, we summarize the recent progress in photoactive nanozyme-based biosensors, including enzyme-like activity regulation, types of photo-responsive biosensors, and mechanism of detection. Although these effective and controllable biosensors had been demonstrated for multiple biomolecule detections, most of these studies were proof-of-concept. Therefore, there is still plenty of room for future development. Several possible opportunities for future improvements have been given as follows. (1) More reaction types of photoactive nanozymes are needed. To date, almost all photoactive nanozyme-based biosensors rely on the oxidase- and peroxidase-like activities, limiting the range of analytes of interest. Since light stimulation is extensively applied in chemical synthesis and biomedical applications, searching for new kinds of photoactive enzyme-like activities for constructing biosensing systems is reasonable and attractive. (2) Using photoactive nanozyme-based sensors for *in vivo* detection. Nanozyme-based *in vitro* sensing systems had been successfully developed, while none of the photo-responsive nanozymes were applied for *in vivo* detection yet. (3) Sensing systems with high selectivity need to be further improved for detection. Substrate specificity is a long-standing challenge for designing nanozymes. Therefore, developing photoactive nanozymes with high specificity for analytes is a promising direction for the construction of biosensors. (4) Developing controllable photoactive sensing systems is attractive for portable detection. The most fascinating feature of light stimulation is that it is controllable, and is useful to control the detection process. However, building controllable detection systems by using photo-responsive nanozymes are limited and difficult. (5) Exploring more nanomaterials with photoactive enzyme-like activity for the development of biosensing systems. The photo-responsive nanozymes are far less than traditional nanozymes and photocatalytic nanomaterials both in quantities and types. We expect that this review will benefit the modulation of light-activated nanozymes and inspire the exploration of more functional photoactive biosensors in future.



## Conflicts of interest

There are no conflicts to declare.

## Acknowledgements

This work was supported by the National Natural Science Foundation of China (21722503 and 21874067), the China Postdoctoral Science Foundation (2019TQ0144 and 2019M661786), the PAPD Program, the Open Funds of the State Key Laboratory of Analytical Chemistry for Life Science (SKLACLS1704), the Open Funds of the State Key Laboratory of Coordination Chemistry (SKLCC1819), and the Fundamental Research Funds for the Central Universities (14380145).

## References

- 1 L. Gao, J. Zhuang, L. Nie, J. Zhang, Y. Zhang, N. Gu, T. Wang, J. Feng, D. Yang, S. Perrett and X. Yan, *Nat. Nanotechnol.*, 2007, **2**, 577–583.
- 2 H. Wei and E. Wang, *Chem. Soc. Rev.*, 2013, **42**, 6060–6093.
- 3 J. Wu, X. Wang, Q. Wang, Z. Lou, S. Li, Y. Zhu, L. Qin and H. Wei, *Chem. Soc. Rev.*, 2019, **48**, 1004–1076.
- 4 D. Jiang, D. Ni, Z. T. Rosenkrans, P. Huang, X. Yan and W. Cai, *Chem. Soc. Rev.*, 2019, **48**, 3683–3704.
- 5 Y. Huang, J. Ren and X. Qu, *Chem. Rev.*, 2019, **119**, 4357–4412.
- 6 J. W. Liu and Y. Lu, *J. Am. Chem. Soc.*, 2003, **125**, 6642–6643.
- 7 Y. Song, K. Qu, C. Zhao, J. Ren and X. Qu, *Adv. Mater.*, 2010, **22**, 2206–2210.
- 8 Y. Lin, J. Ren and X. Qu, *Acc. Chem. Res.*, 2014, **47**, 1097–1105.
- 9 J. C. Colmenares and R. Luque, *Chem. Soc. Rev.*, 2014, **43**, 765–778.
- 10 M. A. Fox and M. T. Dulay, *Chem. Rev.*, 1993, **93**, 341–357.
- 11 M. Anpo and M. Takeuchi, *J. Catal.*, 2003, **216**, 505–516.
- 12 H. Yan, J. Yang, G. Ma, G. Wu, X. Zong, Z. Lei, J. Shi and C. Li, *J. Catal.*, 2009, **266**, 165–168.
- 13 Y. Fu, D. Sun, Y. Chen, R. Huang, Z. Ding, X. Fu and Z. Li, *Angew. Chem., Int. Ed.*, 2012, **51**, 3364–3367.
- 14 B. Jeong and A. Gutowska, *Trends Biotechnol.*, 2002, **20**, 305–311.
- 15 H. Kuhn, *Nature*, 1980, **283**, 587–589.
- 16 C. Tommos and G. T. Babcock, *Acc. Chem. Res.*, 1998, **31**, 18–25.
- 17 B. Schierling, A.-J. Noel, W. Wende, L. T. Hien, E. Volkov, E. Kubareva, T. Oretskaya, M. Kokkinidis, A. Roempp, B. Spengler and A. Pingoud, *Proc. Natl. Acad. Sci. U. S. A.*, 2010, **107**, 1361–1366.
- 18 T. Carell, L. T. Burgdorf, L. M. Kundu and M. Cichon, *Curr. Opin. Chem. Biol.*, 2001, **5**, 491–498.
- 19 J. Xu, Y. Hu, J. Fan, M. Arkin, D. Li, Y. Peng, W. Xu, X. Lin and Q. Wu, *Angew. Chem., Int. Ed.*, 2019, **58**, 8474–8478.
- 20 D. J. Heyes, C. N. Hunter, I. H. M. van Stokkum, R. van Grondelle and M. L. Groot, *Nat. Struct. Biol.*, 2003, **10**, 491–492.
- 21 N. M. Idris, M. K. G. Jayakumar, A. Bansal and Y. Zhang, *Chem. Soc. Rev.*, 2015, **44**, 1449–1478.
- 22 S. Sarina, H. Zhu, E. Jaatinen, Q. Xiao, H. Liu, J. Jia, C. Chen and J. Zhao, *J. Am. Chem. Soc.*, 2013, **135**, 5793–5801.
- 23 F. Wang, C. Li, H. Chen, R. Jiang, L.-D. Sun, Q. Li, J. Wang, J. C. Yu and C.-H. Yan, *J. Am. Chem. Soc.*, 2013, **135**, 5588–5601.
- 24 J. A. Gow and C. D. Manning, *IEEE Proc.: Electr. Power Appl.*, 1999, **146**, 193–200.
- 25 Q. Xiang, B. Cheng and J. Yu, *Angew. Chem., Int. Ed.*, 2015, **54**, 11350–11366.
- 26 Y. Ma, X. Wang, Y. Jia, X. Chen, H. Han and C. Li, *Chem. Rev.*, 2014, **114**, 9987–10043.
- 27 D. Chatterjee and S. Dasgupta, *J. Photochem. Photobiol., C*, 2005, **6**, 186–205.
- 28 X. Liu, L. Jiang, J. Li, L. Wang, Y. Yu, Q. Zhou, X. Lv, W. Gong, Y. Lu and J. Wang, *J. Am. Chem. Soc.*, 2014, **136**, 13094–13097.
- 29 H. Y. Zou, P. F. Gao, M. X. Gao and C. Z. Huang, *Analyst*, 2015, **140**, 4121–4129.
- 30 G. Liu, G. Zhao, W. Zhou, Y. Liu, H. Pang, H. Zhang, D. Hao, X. Meng, P. Li, T. Kako and J. Ye, *Adv. Funct. Mater.*, 2016, **26**, 6822–6829.
- 31 G. Liu, J. Pan, L. Yin, J. T. S. Irvine, F. Li, J. Tan, P. Wormald and H.-M. Cheng, *Adv. Funct. Mater.*, 2012, **22**, 3233–3238.
- 32 N. Waiskopf, Y. Ben-Shahar, M. Galchenko, I. Carmel, G. Moshitzky, H. Soreq and U. Banin, *Nano Lett.*, 2016, **16**, 4266–4273.
- 33 M. Quick, A. L. Dobryakov, M. Gerecke, C. Richter, F. Berndt, I. N. Ioffe, A. A. Granovsky, R. Mahrwald, N. P. Ernstring and S. A. Kovalenko, *J. Phys. Chem. B*, 2014, **118**, 8756–8771.
- 34 M. Irie, *J. Am. Chem. Soc.*, 1983, **105**, 2078–2079.
- 35 C. Wang, Q. Zhang, X. Wang, H. Chang, S. Zhang, Y. Tang, J. Xu, R. Qi and Y. Cheng, *Angew. Chem., Int. Ed.*, 2017, **56**, 6767–6772.
- 36 C. Li, Y. Wang, C. Li, S. Xu, X. Hou and P. Wu, *ACS Appl. Mater. Interfaces*, 2019, **11**, 20770–20777.
- 37 C. Li, Q. Xu, S. Xu, X. Zhang, X. Hou and P. Wu, *RSC Adv.*, 2017, **7**, 16204–16209.
- 38 Y. Zheng, Z. Yu, H. Ou, A. M. Asiri, Y. Chen and X. Wang, *Adv. Funct. Mater.*, 2018, **28**, 1705407.
- 39 M. Sun, L. Xu, A. Qu, P. Zhao, T. Hao, W. Ma, C. Hao, X. Wen, F. M. Colombari, A. F. de Moura, N. A. Kotov, C. Xu and H. Kuang, *Nat. Chem.*, 2018, **10**, 821–830.
- 40 J. Zhang, S. Wu, L. Ma, P. Wu and J. Liu, *Nano Res.*, 2020, **13**, 455–460.
- 41 J. Zhang, X. Lu, D. Tang, S. Wu, X. Hou, J. Liu and P. Wu, *ACS Appl. Mater. Interfaces*, 2018, **10**, 40808–40814.
- 42 M. J. Meziani, X. Dong, L. Zhu, L. P. Jones, G. E. LeCroy, F. Yang, S. Wang, P. Wang, Y. Zhao, L. Yang, R. A. Tripp

- and Y.-P. Sun, *ACS Appl. Mater. Interfaces*, 2016, **8**, 10761–10766.
- 43 X. Xie, C. Mao, X. Liu, Y. Zhang, Z. Cui, X. Yang, K. W. K. Yeung, H. Pan, P. K. Chu and S. Wu, *ACS Appl. Mater. Interfaces*, 2017, **9**, 26417–26428.
  - 44 C. M. Courtney, S. M. Goodman, J. A. McDaniel, N. E. Madinger, A. Chatterjee and P. Nagpal, *Nat. Mater.*, 2016, **15**, 529–534.
  - 45 J. Zhang and J. Liu, *Nanoscale*, 2020, **12**, 2914–2923.
  - 46 S. Wu, J. Zhang and P. Wu, *Anal. Methods*, 2019, **11**, 5081–5088.
  - 47 W. Bi, X. Li, L. Zhang, T. Jin, L. Zhang, Q. Zhang, Y. Luo, C. Wu and Y. Xie, *Nat. Commun.*, 2015, **6**, 8647.
  - 48 J. Li, X. Liu, L. Tan, Y. Liang, Z. Cui, X. Yang, S. Zhu, Z. Li, Y. Zheng, K. W. K. Yeung, X. Wang and S. Wu, *Small Methods*, 2019, **3**, 1900048.
  - 49 P. Zhang, T. Wang, X. Chang and J. Gong, *Acc. Chem. Res.*, 2016, **49**, 911–921.
  - 50 F. D'Souza and O. Ito, *Chem. Soc. Rev.*, 2012, **41**, 86–96.
  - 51 J. Zhang, S. Wu, X. Lu, P. Wu and J. Liu, *Nano Lett.*, 2019, **19**, 3214–3220.
  - 52 C. Wang, Y. Shi, Y.-Y. Dan, X.-G. Nie, J. Li and X.-H. Xia, *Chem. – Eur. J.*, 2017, **23**, 6717–6723.
  - 53 F. Su, S. C. Mathew, G. Lipner, X. Fu, M. Antonietti, S. Blechert and X. Wang, *J. Am. Chem. Soc.*, 2010, **132**, 16299–16301.
  - 54 R. Wang, B. Li, Y. Xiao, X. Tao, X. Su and X. Dong, *J. Catal.*, 2018, **364**, 154–165.
  - 55 X. Sun, X. Luo, X. Zhang, J. Xie, S. Jin, H. Wang, X. Zheng, X. Wu and Y. Xie, *J. Am. Chem. Soc.*, 2019, **141**, 3797–3801.
  - 56 H. M. D. Bandara and S. C. Burdette, *Chem. Soc. Rev.*, 2012, **41**, 1809–1825.
  - 57 J. Tamogami, T. Kikukawa, T. Nara, K. Shimono, M. Demura and N. Kamo, *Biochemistry*, 2012, **51**, 9290–9301.
  - 58 H. K. Moon, S. H. Lee and H. C. Choi, *ACS Nano*, 2009, **3**, 3707–3713.
  - 59 F. Wang, E. Ju, Y. Guan, J. Ren and X. Qu, *Small*, 2017, **13**, 1603051.
  - 60 F. Wang, Y. Zhang, Z. Du, J. Ren and X. Qu, *Nat. Commun.*, 2018, **9**, 1209.
  - 61 S. Neri, S. G. Martin, C. Pezzato and L. J. Prins, *J. Am. Chem. Soc.*, 2017, **139**, 1794–1797.
  - 62 S. Laimgruber, T. Schmierer, P. Gilch, K. Kiewisch and J. Neugebauer, *Phys. Chem. Chem. Phys.*, 2008, **10**, 3872–3882.
  - 63 X. Wang, A. Gong, W. Luo, H. Wang, C. Lin, X. Y. Liu and Y. Lin, *Chem. Commun.*, 2018, **54**, 8641–8644.
  - 64 J. Niu, Y. Sun, F. Wang, C. Zhao, J. Ren and X. Qu, *Chem. Mater.*, 2018, **30**, 7027–7033.
  - 65 L. Fan, X. Xu, C. Zhu, J. Han, L. Gao, J. Xi and R. Guo, *ACS Appl. Mater. Interfaces*, 2018, **10**, 4502–4511.
  - 66 F. Yesilkoy, R. A. Terborg, J. Pello, A. A. Belushkin, Y. Jahani, V. Pruneri and H. Altug, *Light: Sci. Appl.*, 2018, **7**, 17152.
  - 67 V. K. Johns, P. K. Patel, S. Hassett, P. Calvo-Marzal, Y. Qin and K. Y. Chumbimuni-Torres, *Anal. Chem.*, 2014, **86**, 6184–6187.
  - 68 J. Kim, S. Lee, K. Jung, W. C. Oh, N. Kim, S. Son, Y. Jo, H.-B. Kwon and W. D. Heo, *Nat. Commun.*, 2019, **10**, 211.
  - 69 Y. Jin, *Adv. Mater.*, 2012, **24**, 5153–5165.
  - 70 Y. Shiraishi, K. Adachi, M. Itoh and T. Hirai, *Org. Lett.*, 2009, **11**, 3482–3485.
  - 71 F. Nourmohammadian, T. Wu and N. R. Branda, *Chem. Commun.*, 2011, **47**, 10954–10956.
  - 72 N. Shao, J. Y. Jin, S. M. Cheung, R. H. Yang, W. H. Chan and T. Mo, *Angew. Chem., Int. Ed.*, 2006, **45**, 4944–4948.
  - 73 V. Valderrey, A. Bonasera, S. Fredrich and S. Hecht, *Angew. Chem., Int. Ed.*, 2017, **56**, 1914–1918.
  - 74 W.-W. Zhao, J.-J. Xu and H.-Y. Chen, *Chem. Soc. Rev.*, 2015, **44**, 729–741.
  - 75 C. Feng, D. Chan, J. Joseph, M. Muuronen, W. H. Coldren, N. Dai, I. R. Correa Jr., F. Furche, C. M. Hadad and R. C. Spitale, *Nat. Chem. Biol.*, 2018, **14**, 276–283.
  - 76 G.-L. Wang, X.-F. Xu, L. Qiu, Y.-M. Dong, Z.-J. Li and C. Zhang, *ACS Appl. Mater. Interfaces*, 2014, **6**, 6434–6442.
  - 77 G.-L. Wang, L.-Y. Jin, Y.-M. Dong, X.-M. Wu and Z.-J. Li, *Biosens. Bioelectron.*, 2015, **64**, 523–529.
  - 78 D. Wu, N. Hu, J. Liu, G. Fan, X. Li, J. Sun, C. Dai, Y. Suo, G. Li and Y. Wu, *Talanta*, 2018, **190**, 103–109.
  - 79 L.-Y. Jin, Y.-M. Dong, X.-M. Wu, G.-X. Cao and G.-L. Wang, *Anal. Chem.*, 2015, **87**, 10429–10436.
  - 80 G.-L. Wang, X.-Q. Li, G.-X. Cao, F. Yuan, Y. Dong and Z. Li, *Chem. Commun.*, 2017, **53**, 11165–11168.
  - 81 G.-L. Wang, X. Xu, X. Wu, G. Cao, Y. Dong and Z. Li, *J. Phys. Chem. C*, 2014, **118**, 28109–28117.
  - 82 Y. Guo, X. Li, Y. Dong and G.-L. Wang, *ACS Sustainable Chem. Eng.*, 2019, **7**, 7572–7579.
  - 83 P. Zhang, D. Sun, A. Cho, S. Weon, S. Lee, J. Lee, J. W. Han, D.-P. Kim and W. Choi, *Nat. Commun.*, 2019, **10**, 940.
  - 84 Y. Liu, M. Zhou, W. Cao, X. Wang, Q. Wang, S. Li and H. Wei, *Anal. Chem.*, 2019, **91**, 8170–8175.
  - 85 H. S. White, W. G. Becker and A. J. Bard, *J. Phys. Chem.*, 1984, **88**, 1840–1846.